Hindawi
Mathematical Problems in Engineering
Volume 2020, Article ID 7083639, 12 pages
https://doi.org/10.1155/2020/7083639

Research Article

U-Model-Based Finite-Time Control for Nonlinear Valve-Controlled Hydraulic Servosystem

Hao Yan[1,2] **Jiafeng Li**[1] **Hassan Nouri**[3] **and Lingling Xu**[1]

[1]*School of Mechanical, Electronic and Control Engineering, Beijing Jiaotong University, Beijing 100044, China*
[2]*Key Laboratory of Vehicle Advanced Manufacturing, Measuring and Control Technology, Beijing Jiaotong University, Ministry of Education, Beijing 100044, China*
[3]*Power System and Control Research Laboratory, University of the West of England, Bristol BS16 1QY, UK*

Correspondence should be addressed to Hao Yan; hyan@bjtu.edu.cn

Received 25 November 2019; Accepted 4 January 2020; Published 10 February 2020

Guest Editor: Weicun Zhang

Valve-controlled servosystems are widely used in dynamic tracking, but, not properly studied, nonlinearity, perturbation of internal parameters, and external disturbance have significant impacts on the control performance and challenge in the controller design. This study, with consideration of the finite pressure gain of actual servovalves, proposes a new unified nonlinear model of the valve-controlled servosystem. Based on a U-control platform, this study makes the control strategy design independent from the nonlinear plant, and a virtual nominal plant is presented to eliminate the unmodeled high-frequency characteristics, acquire the desired control performance, and enable the control variable to be explicitly expressed. Then, there follows, designing the *U*-model-based finite-time control in the valve-controlled systems. Simulation demonstrations show the consistency with theoretical development that the valve-controlled system can smoothly track the command signal within the specified time, and the phase lag is eliminated. Moreover, *U*-model's application effectively copes with the system chattering, and with the maximum of 1 m/s the dynamic position error caused by discretization of the controller is reduced to less than 0.15%, which can satisfy the demand of general valve-controlled servosystems.

1. Introduction

With the advantages of fast response and high stiffness, valve-controlled servosystems have been widely applied in machinery manufacturing, ship maneuvering, and industrial control. The traditional valve-controlled system often adopts output feedback and the PID control method to achieve dynamic tracking. However, almost all the valve-controlled systems work based on the throttle mechanism and the working pressure produced by closed chambers. Therefore, inherent nonlinear elements exist. With the increase of the spool deviation and the movement of the actuator, not only the nonlinear throttling effect becomes remarkable but also the structural parameters of the hydraulic actuator vary. Particularly, the orifices exhibit different directional properties in valve forward and reverse. Actually, for strongly dynamic signals, the tracking effect of the valve-controlled system is often unsatisfactory, involving phenomena of lag and attenuation. In addition, parameter uncertainties and external disturbances also play a complicated role in degrading the valve-controlled system operation. Consequently, for improving control performance, new research and development should expand those developed from linear model-based approaches that treat the valve-controlled systems as a linear system and simplify it into a second-order oscillating element.

The traditional controller design of the valve-controlled servosystem is based on the linearization of the hydraulic drive mechanism and frequency domain analyses [1–3], forming a set of linear theoretical methods and focusing on the valve control system's applications in engineering. To adapt to the advanced control algorithm and enhance the dynamic performance further, building up a nonlinear state space model and pursuing the finite transitional time become important research topics. Although the finite-time control has been developed in some tracking applications in recent years [4–8], it is seldom appeared in valve-controlled systems due to the difficulty of constructing a reasonable model for this nonlinear system. Ye [9] established different nonlinear state space models for different directions of the orifice and linearized them, respectively. Based on nonlinear models of the valve-controlled system, Li et al. [10] built an adaptive sliding mode controller. In this system, the fuzzy algorithm is used to estimate the equivalent control and the genetic algorithm is used to realize the adaptive switching control. And Li et al. [11] applied the second-order sliding mode control method in the valve-controlled system and scheduled the reaching speed with the optimization objective of time, which is substantially a finite-time controller. Schmidt et al. [12] clearly presented a finite-time controller for the linearized valve-controlled system by utilizing a modified super-twisting controller. Moreover, adopting the terminal sliding mode control method, Yao et al. [13] proposed a finite-time controller for the nonlinear valve-controlled system. In a critical comment of these aforementioned studies, the nonlinear models are all variable structure models depending on the polarity of the valve's control variable, which is only an ideal situation and inconsistent with the actual system. And since the control variable cannot be expressed explicitly, the discontinuity and mismatching caused by the control variable could only be treated as uncertainty, and the global robustness to initial states was not considered. These factors have restricted further improvement of the finite-time controller for valve-controlled systems.

In fact, to reduce the complexity of the model-based control system design, particularly for those nonlinear dynamic plants, Zhu [14–16] proposed a systematical universal transform to convert classical nonlinear polynomial models into U-models with time-varying parameters and controller output $u(t-1)$. This U-model-based control design framework, U-control in short, and it stands for <model independent design> against conventional <model based design> and <model free (data driven) design>. In the design, no matter what kind of the plant model structure is, like linear/nonlinear or polynomial/state space, U-control separates the closed-loop control system design from controller output determination, accordingly a linear control performance with dynamic and steady state requests can be specified with damping ratio and undamped natural frequency. For determining the controller output, the plant U-model is referred facilitating dynamic inversion in root solving. It should be noted that U-control is not aiming at increasing control accuracy; it is, indeed, for improving design feasibility and efficiency in concise formulation. As it is a supplement to the classical model-based control framework, U-control can integrate well-developed linear control system design approaches with nonlinear dynamic plants.

The major contributions of the study include

(1) Deriving a proper principle model to accommodate dynamic and nonlinearities for a typical valve-controlled servosystem

(2) Using U-control to separate control system design and controller output determination

(3) Developing a global robust sliding mode control scheme for valve-controlled systems

(4) Providing computational experiments to validate the control scheme and to guide the potential users in their potential ad hoc applications

The rest of the study is organised into five sections. Section 1 establishes the nonlinear model of a typical valve-controlled system. After analysis on the model variable structure, it reformulates a more practical and unified nonlinear model. Section 2 derives the U-model realization of the principle model developed in Section 1, which is used for the dynamic inversion of the valve-controlled system and proposes a virtual nominal plant model to eliminate the unmodeled high-frequency dynamics and achieve the performance objective. Section 3 derives a global robust finite-time controller based on U-control platform. Section 4 provides simulation studies to demonstrate the feasibility of the proposed controller procedure, in addition to provide guidance for potential users for their ad hoc expansions/applications. Finally, Section 5 concludes the study.

2. Modeling of Valve-Controlled Servosystems

Figure 1 shows a typical valve-controlled system consists of four-way spool valves and a symmetrical hydraulic actuator. The hydraulic oil is throttled twice from the inlet and outlet, and then the pressure is formed in the left and right chambers of the cylinder. The pressure difference between the two chambers is the working pressure, which drives the piston for load motion. Generally, the load includes inertia, elastic and viscous components, and other arbitrary components can be thought of as external disturbances.

Assuming that the fluid is incompressible, it can formulate the valve-controlled system as [2]

$$Q_L = C_d w_x x_v \sqrt{\frac{1}{\rho}\left(P_s - \operatorname{sgn}(x_v) P_L\right)}, \tag{1}$$

$$Q_L = A\dot{y} + C_{\mathrm{te}} P_L + \frac{V_t}{4\beta_e}\dot{P}_L, \tag{2}$$

$$AP_L = m\ddot{y} + B_c\dot{y} + Ky + F, \tag{3}$$

where x_v: the displacement of the spool, P_L: the working pressure. A: the effective area of the piston, y: the displacement of the piston, β_e: the elastic modulus of oil, V_t: the total volume of the two chambers of the cylinder, m: the total mass of the piston, B_c: the damping coefficient of the load, K: the spring stiffness of the load, F: the arbitrary external load acting on the piston, C_d: the flow coefficient of the throttle, w_x: the area gradient of the orifice, P_s: the supply pressure of the oil, ρ: the density of the oil, and C_{te}: the total leaking coefficient calculated by $C_{\mathrm{te}} = C_{\mathrm{ic}} + C_{\mathrm{ec}}$ in which C_{ic} and C_{ec} are the internal leaking coefficient and external leaking coefficient, respectively.

From equations (1) and (2), it gives

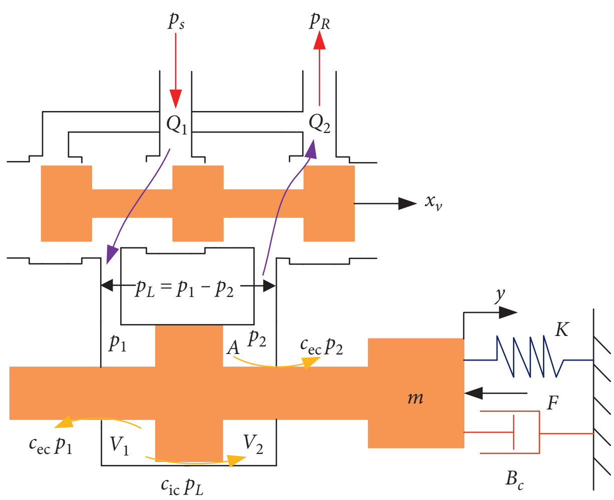

FIGURE 1: Valve-controlled system's structure.

$$A\dot{y} + C_{te}P_L + \frac{V_t}{4\beta_e}\dot{P}_L = C_d w_x x_v \left(\frac{1}{\rho}\left(P_s - \text{sgn}\left(x_v\right)P_L\right)\right)^{1/2}. \tag{4}$$

(3) and its derivative give the following set equations:

$$P_L = \frac{1}{A}\left(m\ddot{y} + B_c\dot{y} + Ky + F\right), \tag{5}$$

$$\dot{P}_L = \frac{1}{A}\left(m\dddot{y} + B_c\ddot{y} + K\dot{y} + \dot{F}\right). \tag{6}$$

Substituting equations (5) and (6) into equation (4) yields

$$\begin{aligned}\dddot{y} = &-\left(\frac{C_{te}}{b} + \frac{B_c}{m}\right)\ddot{y} - \frac{A^2 + C_{te}B_c + bK}{bm}\dot{y} - \frac{C_{te}K}{bm}y \\ &-\left(\frac{C_{te}}{bm}F + \frac{1}{m}\dot{F}\right) + \Psi\left(x_v, y, F\right),\end{aligned} \tag{7}$$

where $\Psi(x_v, y, F) = ((AC_d w_x\sqrt{(1/\rho)})/bm)\ (P_s - \text{sgn}(x_v)\ (1/A)(m\ddot{y} + B_c\dot{y} + Ky + F))^{1/2}x_v$ and $b = (V_t/4\beta_e)$.

Choosing the state variables as

$$\begin{cases} x_1 = y, \\ x_2 = \dot{x}_1 = \dot{y}, \\ x_3 = \dot{x}_2 = \ddot{y}, \end{cases} \tag{8}$$

and assigning the control variable $u = x_v$, it gives the state space representation of the nonlinear dynamic model, which will facilitate the following control system designs:

$$\begin{cases} \dot{x}_1 = x_2, \\ \dot{x}_2 = x_3, \\ \dot{x}_3 = \left(\frac{c_{te}}{b} + \frac{B_c}{m}\right)x_3 - \frac{A^2 + c_{te}B_c + b_K}{bm}x_2 - \frac{c_{te}K}{bm}x_1 \\ \quad -\left(\frac{c_{te}}{bm}F + \frac{1}{m}\dot{F}\right) + \Psi\left(u, \mathbf{x}, F\right), \end{cases} \tag{9}$$

$$y = x_1,$$

where

$$\begin{aligned}\Psi(u, \mathbf{x}, F) = \frac{AC_d w_x\sqrt{(1/\rho)}}{bm}\Big(P_s - \text{sgn}(u)\frac{1}{A}(mx_3 \\ + B_c x_2 + Kx_1 + F)\Big)^{1/2}u,\end{aligned} \tag{10}$$

and $\mathbf{x} = [x_1, x_2, x_3]^T$.

The state space model (9) can be abbreviated as

$$\begin{cases} \dot{x}_1 = x_2, \\ \dot{x}_2 = x_3, \\ \dot{x}_3 = f(\mathbf{x}) + \Psi(u, \mathbf{x}, F) + \text{d}(F), \end{cases} \tag{11}$$
$$y = x_1,$$

where $f(\mathbf{x}) = -(C_{te}/b + B_c/m)x_3 - ((A^2 + C_{te}B_c + bK)/bm)\ x_2 - (C_{te}K/bm)x_1$ is the linear item of the system, $\Psi(u, \mathbf{x}, F)$ is a nonlinear function augmented with the control variable, the external force, and the state vector, and $\text{d}(F) = -((C_{te}/bm)F + (1/m)\dot{F})$ is the disturbance related to the external force.

Inspection of equation (10), there exists a sign function in $\Psi(u, \mathbf{x}, F)$ and the load pressure difference is $\text{sgn}(u)(1/A)(mx_3 + B_c x_2 + Kx_1 + F)$, which means that the pressure gain is infinity while u tends to zero displacement of the spool. This is just an ideal and extreme condition. However, this assumption is not consistent with the actual scenarios and it has led to a variable structure and noncontinuous feature for different polarities of the control variable. In fact, because the radial clearance between the spool and the sleeve always exists, the actual pressure gain is a finite value. The experimental pressure gain curve of the servovalve is given by Reference [2]. Alternatively, it can be deduced that when the servovalve's control variable changes polarity, the load pressure will change along the pressure gain curve, not a step function. Then, according to the characteristics of the experimental curve, this study proposes replacing the sign function with a hyperbolic tangent function to describe the pressure difference state, as depicted in Figure 2, which can bring the same motion pattern as the experimental pressure.

Then, equation (10) becomes

$$\begin{aligned}\Psi(u, x, F) = \frac{AC_d w_x\sqrt{(1/\rho)}}{bm}\Big(P_s - \tanh(\lambda u)\frac{1}{A}(mx_3 + B_c x_2 \\ + Kx_1 + F)\Big)^{1/2}u,\end{aligned} \tag{12}$$

where $\tanh(\lambda u) = (e^{\lambda \mu} - e^{-\lambda \mu})/(e^{\lambda \mu} + e^{-\lambda \mu})$ and λ is a real constant greater than 1. The value of λ should make the pressure gain consistent with the experimental value. Consequently, equations (11) and (12) constitute a unified smooth nonlinear model for valve-controlled systems.

3. Using *U*-Control to Separate Control System Design and Controller Output Determination

3.1. U-Model Realization of Valve-Controlled Servosystem. Usually, the continuous smooth system, including linear and nonlinear systems, can be formulated as a polynomial

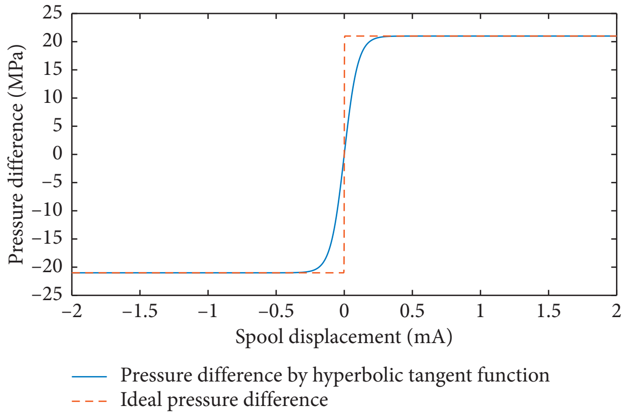

Figure 2: Load pressure difference near the zero displacement of the spool.

function with time-varying parameters, i.e., NARMAX (Nonlinear Autoregressive Moving Average with Exogenous input) model [17]. Without losing generality, consider a Single Input Single Output (SISO) U-model for a general discrete time nonlinear system with respect to output $y(k)$ and control input $u(k-1)$ [15]:

$$y(k) = \sum_{j=0}^{M} \lambda_j(k) u^j(k-1), \tag{13}$$

where $u \in \mathbb{R}^1$ is the input, $y \in \mathbb{R}^1$ is the output, M is the degree of the input, the time-varying parameter vector $\lambda(k) = [\lambda_0(k), \cdots, \lambda_M(k)] \in \mathbb{R}^{M+1}$ is a function of past inputs and outputs $(u(k-2), \ldots, u(k-n), y(k-1), \ldots, y(k-n))$, and k is the sampling instance.

The input and output dynamic relationship of equation (13) can be expressed as a map of

$$U\colon u(k-1) \longrightarrow y(k). \tag{14}$$

Customarily, this map is called U-model realization of the system. If the inverse of the map exists, it has

$$U^{-1}\colon y(k) \longrightarrow u(k-1). \tag{15}$$

On this basis, a U-model-based controller framework can be established as

$$\sum_{U \text{ Framework}} = (\Phi \;\; U^{-1}), \tag{16}$$

where Φ is the closed-loop control algorithm and it can be any linear time-invariant control method. For example, for PID control, it includes error calculation and a PID module. U^{-1} represents the inversion operation for the U-model. Figure 3 illustrates this framework.

Because the plant amounts to the map U, if the inversion of the U-model is accurate, the output of the controller $u(k-1)$ will ensure that the actual output $y(k)$ is equal to the desirable output $y_d(k)$. Thus, the effect of the nonlinear characteristics on the controller design can be cancelled ideally and the design of control algorithm is made independent from the nonlinear system. Accordingly, all off-the-shelf and advanced control strategies for linear systems can be applied to a variety of nonlinear systems.

The U-model control method brings the following advantages. Firstly, this is a model-independent controller design framework, which can polish the complex plant model and freely give the system the required closed-loop dynamic performance by various control strategies. Secondly, the traditional design of the nonlinear control system is decomposed into control algorithm design and real-time dynamic inversion. These processes can be carried out in parallel, which greatly improves the design efficiency and reduces the design difficulty. Thirdly, this method has versatility, that is, it is suitable for not only nonlinear systems but also complex linear systems, and almost all known control strategies can be applied in the closed-loop control algorithm. At last, the interchangeability of the controller design is realized. For the satisfactory control algorithm, when the plant changes only the U-model needs to be updated to ensure the invariant performance of the system.

However, for most nonlinear systems, it is difficult to obtain the analytical solution by U-model. Therefore, the realization of U-model method depends on solving the inverse of the U-model numerically for each sampling period, which is naturally discrete and practical for engineering. So the discretization of the nonlinear plant's model is needed firstly. According to the characteristics of equation (11), the first-order backward difference method is used to discretize the system as follows:

$$\begin{cases} x_1(k) = x_1(k-1) + hx_2(k), \\ x_2(k) = x_2(k-1) + hx_3(k), \\ x_3(k) = x_3(k-1) + h\{f[x(k)] + d[F(k)] + \Psi[u(k), x(k), F(k)]\}, \end{cases} \tag{17}$$
$$y(k) = x_1(k),$$

where h is the sampling period. Equation (17) can be seen as a generalized U-model in the form of state equations. When $x_1(k)$ is given, the solutions of $x_2(k)$ and $x_3(k)$ can be derived by backstepping routines, and finally the control variables $u(k)$ can be obtained by solving the nonlinear equation. For a valve-controlled system described by

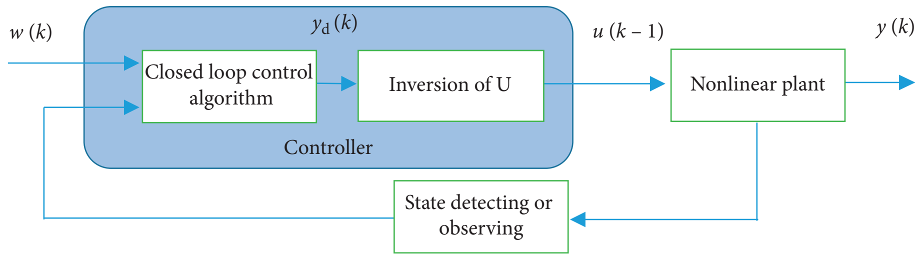

FIGURE 3: *U*-model method frame.

equation (17), the solution will be $u(k)$ rather than $u(k-1)$ because the function Ψ is a complex nonlinear function with respect to $u(k)$. Meanwhile, the *U*-model cannot be written as a time-varying coefficient polynomial such as the classical *U*-model. Consequently equation (17) can be regarded as an extension of *U*-model, and $u(k)$ can still be solved numerically by the Newton–Raphson method as

$$u_{n+1}(k) = u_n(k) - \frac{x_3(k) - x_3[u_n(k)]}{(\mathrm{d}[x_3(k)]/\mathrm{d}u(k))}, \tag{18}$$

where n is the number of iterations. According to equation (14), in order to realize the inversion of the nonlinear model, $\mathrm{d}[x_3(k)]/\mathrm{d}u(k)$ is needed to be updated continuously, which requires that the function $x_3(k)$ is first-order differentiable with respect to $u(k)$. According to equations (12) and (17), this requirement can be satisfied. Because the parameters in the expression of $x_3(k)$ are time-varying, we can firstly take a derivative of its symbolic expression in the computer for each sampling period and then calculate current $\mathrm{d}[x_3(k)]/\mathrm{d}u(k)$ and $u_{n+1}(k)$. For example, giving a sinusoidal signal to a valve-controlled hydraulic system as the desirable output $y_d(k)$, we can perform simulation according to equations (17) and (18) with the parameters specified by Table 1. The output of controller $u(k)$ and the system response $y(k)$ are shown in Figures 4 and 5, respectively. The simulation shows that under ideal conditions the output of the controller u is stable and smooth after an initial transient vibration, and the dynamic performance of the valve-controlled system is perfectly compensated by solving the inverse numerically.

3.2. Design of Fundamental Performance of Valve-Controlled System. Ideally, the inverse of the nonlinear system can accurately to eliminate the influence of the nonlinear plant on the design of controllers. However, in reality, it is impossible to obtain perfect results over the full frequency band, since there always exist high-frequency external disturbance and unmodeled dynamics. Therefore, besides the introduction of a closed-loop algorithm, it is necessary to design a suitable filter to inhibit these unfavorable conditions in the high-frequency range. In addition, it can also cancel undesirable high-frequency excitations and noises. In fact, this filter can be regarded as a virtual nominal plant, which will assist in the design of the closed-loop controller and determine the fundamental performance of the system. Figure 6 shows the structure of *U*-control based on the output feedback and the virtual nominal system.

The virtual nominal plant is separated from the control algorithm, which enables to specify an open-loop performance G_V for the plant within a certain range, and any ready-made controller G_c can be adopted. Consequently, for different nonlinear plants, an identical control strategy and the same performance can be achieved conveniently, and the repeated controller design process can be omitted so that the design efficiency is greatly enhanced. Therefore, different from the traditional model-based or model free controller design methods, the *U*-model method including a virtual nominal plant is a model-independent design scheme and provides an interface for various algorithms and various performances developed from model classical approaches.

Moreover, if the specified closed-loop performance is W_b and $G = G_c G_V$ is defined as the open-loop characteristic of the entire system, we can obtain G by

$$G = \frac{W_b}{1 - W_b}. \tag{19}$$

Then, applying G to the digital controller, the expected dynamic performance can be achieved. Typically, valve-controlled servosystems [2] can be considered as a third-order linear system with the closed-loop transfer function:

$$W_b(s) = \frac{1}{((1/\omega_b)s + 1)((1/\omega_{\mathrm{nc}}^2)s^2 + (2\xi_{nc}/\omega_{\mathrm{nc}})s + 1)}, \tag{20}$$

where ω_b is the bandwidth of the system, ω_{nc} is the resonance frequency, and ξ_{nc} is the damping ratio. Assuming that the closed-loop performance W_b is the design objective, according to equation (19) the open-loop performance G can be expressed by

$$G = \frac{1}{\beta_3 s^3 + \beta_2 s^2 + \beta_1 s}, \tag{21}$$

where $\beta_3 = 1/(\omega_b \omega_{\mathrm{nc}}^2)$, $\beta_2 = 2\xi_{\mathrm{nc}}/(\omega_b \omega_{\mathrm{nc}}^2) + 1/\omega_{\mathrm{nc}}^2$, and $\beta_1 = 1/\omega_b + 2\xi_{\mathrm{nc}}/\omega_{\mathrm{nc}}$. Thus, in the controller, the relationship between y_d and the control error e_r can be expressed as

$$\sum_{i=1}^{3} \beta_i y_d^{(i)}(t) = e_r(t). \tag{22}$$

After discretizing equation (22) by a certain method, the digital controller in Figure 6 can be determined, and the nonlinear valve-controlled servosystem will obtain the performance of the specified three-order linear system, that can be considered as a fundamental performance for further

Table 1: Parameters of simulated valve-controlled system.

Parameters	Symbol	Value
Total leakage coefficient	C_{te}	2×10^{-13} (m^3/s/Pa)
Total volume of cylinder	V_t	1.72×10^{-3} (m^3)
Total mass of piston	m	80 (Kg)
Effective area of piston	A	3.44×10^{-3} (m^2)
Elastic modulus of oil	β_e	6.9×10^{8} (Pa)
Flow coefficient of throttle	C_d	0.69
Density of the oil	ρ	880 (Kg/m^3)
Oil supply's pressure	P_s	21 (MPa)
Damping coefficient	B_c	1000 (N/(m/s))
	c_1	4
Parameters of switching surface	c_2	4
	c_3	1
Resonance frequency	ω_{nc}	20 (Hz)
Bandwidth of the system	ω_b	8 (Hz)
Damping ratio	ξ_{nc}	0.7
Coefficient of hyperbolic tangent	λ	12
Error limit	D_1	0.01
Error limit	D_2	0.1
Specified finite time	T	3 (s)

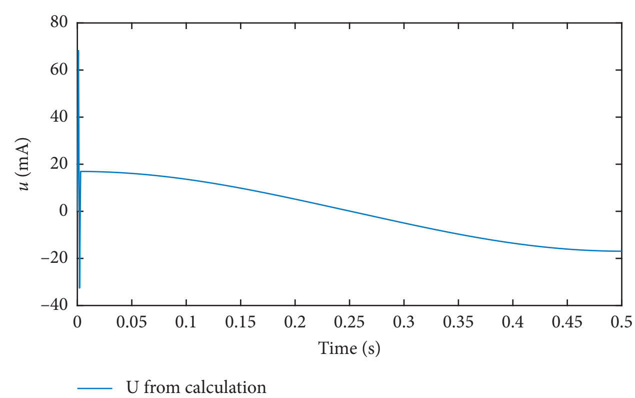

Figure 4: Output of controller $u(k)$.

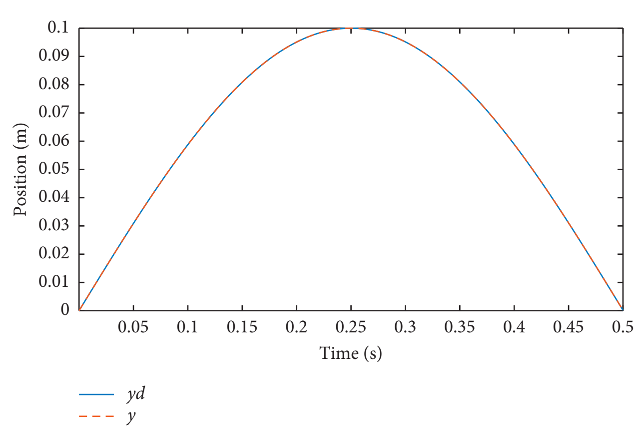

Figure 5: Desirable output $y_d(k)$ and the system response $y(k)$.

processing. In fact, W_b can be the model of any simpler systems, even other types of transmission mechanisms, and this flexibility will enable the valve-controlled system to replace the other types of actuators conveniently.

4. *U*-Model-Based Finite-Time Controller

For the nonlinear valve-controlled servosystem represented by equations (11) and (12), the control variable cannot be expressed explicitly, leading to difficulty for applying general control strategies. However, by the *U*-model method, the nonlinearity of the system is removed by its inversion, which makes it possible to further improve the performance of the system. For valve-controlled hydraulic servosystems, the general requirement is fast response and perfect tracking, but the initial state is usually arbitrary, which often leads to violent vibration caused by excessive control variable. Therefore, the *U*-model-based finite-time control with global robustness is proposed for valve-controlled systems.

As mentioned above, transform the nonlinear valve-controlled servosystem into a new equivalent linear system with dynamic performance W_b, as shown in Figure 7.

The state variables of the new system are still defined by equation (8), and then the state equations are

$$\begin{cases} \dot{x}_1 = x_2, \\ \dot{x}_2 = x_3, \\ \dot{x}_3 = -\dfrac{\beta_2}{\beta_3}x_3 - \dfrac{\beta_1}{\beta_3}x_2 - x_1 + \dfrac{1}{\beta_3}w(t), \end{cases} \quad (23)$$
$$y = x_1.$$

Assuming that the state vector $\mathbf{x} = [x_1, x_2, x_3]^T$ and the given desirable state vector $\mathbf{x}_d = [x_{1d}\, x_{2d}, x_{3d}]^T$, where $x_{2d} = \dot{x}_{1d}$ and $x_{3d} = \ddot{x}_{1d}$, and the error vector can be calculated by

$$\mathbf{e}(t) = \mathbf{x} - \mathbf{x}_d = [e_1, e_2, e_3]^T, \quad (24)$$

where e_1 is the displacement error, $e_2 = \dot{e}_1$ and $e_3 = \ddot{e}_1$.

For the valve-controlled system, the error $\mathbf{e}$ is taken as the state vector to design the switching function. According to a definition [18] and extending the method to third-order case, the global sliding mode surface has a general form as

$$s = c_1 e_1 + c_2 e_2 + c_3 e_3 - p_f(t), \quad (25)$$

where $c_i\,(i = 1, 2, 3)$ is the positive real constant ensuring that $c_3\tau^2 + c_2\tau + c_1$ is a stable Hurwitz polynomial, in which τ is the Laplace operator, and $p_f(t)$ is a forcing function, determining the dynamic of the switching surface. For the existence of the switching surface, $p_f(t)$ must be first-order differentiable. Assuming that

$$p_f(t) = c_1 p_1(t) + c_2 p_2(t) + c_3 p_3(t), \quad (26)$$

when the system works on the switching surface,

$$s = c_1(e_1 - p_1) + c_2(e_2 - p_2) + c_3(e_3 - p_3) = 0. \quad (27)$$

That is,

$$s = \mathbf{c}\cdot[\mathbf{e}(t) - \mathbf{p}(t)] = 0, \quad (28)$$

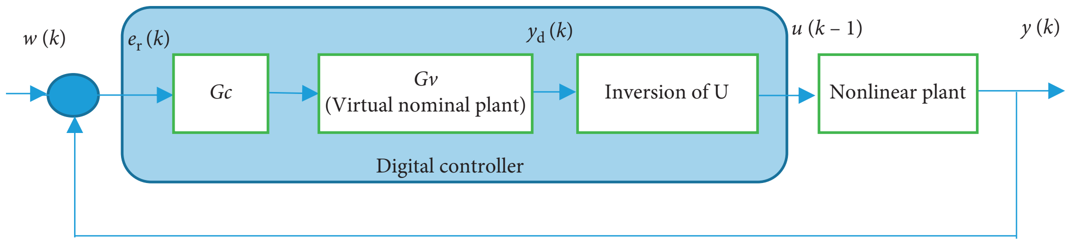

FIGURE 6: *U*-model method including virtual nominal plant.

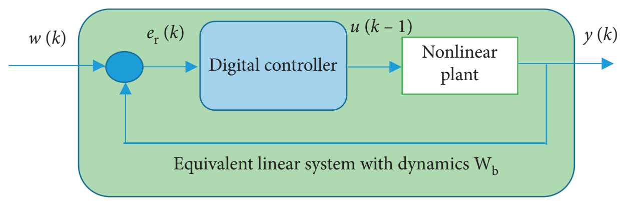

FIGURE 7: *U*-model-based equivalent system.

where $\mathbf{c} = [c_1, c_2, c_3]^T$, $\mathbf{p}(t) = [p_1(t), p_2(t), p_3(t)]^T$, and $p_f(t) = \mathbf{c} \cdot \mathbf{p}(t)$.

Because $e_2 = \dot{e}_1$ and $e_3 = \ddot{e}_1$, it should be ensured that $p_2 = \dot{p}_1$ and $p_3 = \dot{p}_2 = \ddot{p}_1$ in order to satisfy equation (27). Then, if the state vector $\mathbf{e}$ is needed to converge to zero in the finite time T, equation (23) must be satisfied with the following boundary conditions. That is, if $t = 0$, $p_1(0) = e_1(0)$, $p_2(0) = \dot{p}_1(0) = \dot{e}_1(0)$, $p_3(0) = \ddot{p}_1(0) = \ddot{e}_1(0)$, and $\dot{p}_3(0) = \dddot{p}_1(0) = \dddot{e}_1(0)$. And if $t = T$, $p_1(T) = e_1(T) = 0$, $p_2(T) = \dot{p}_1(T) = 0$, $p_3(T) = \ddot{p}_1(T) = 0$, and $\dot{p}_3(T) = \dddot{p}_1(T) = 0$. For these eight equations, a sever-order polynomial can be designed to construct $p_1(t)$

$$p_1(t) = \begin{cases} a_0 + a_1 t + a_2 t^2 + a_3 t^3 + a_4 t^4 + a_5 t^5 + a_6 t^6 + a_7 t^7, & 0 \le t < T, \\ 0, & t \ge T. \end{cases} \tag{29}$$

Substituting the boundary conditions into equation (29), $p_1(t)$ can be obtained as

$$\begin{cases} e_1(0) + \dot{e}_1(0) + \dfrac{1}{2}\ddot{e}_1(0)t^2 + \dfrac{1}{6}\dddot{e}_1(0)t^3 + \left[\dfrac{-35}{T^4}e_1(0) + \dfrac{-20}{T^3}\dot{e}_1(0) + \dfrac{-5}{T^2}\ddot{e}_1(0) + \dfrac{-2}{3T}\dddot{e}_1(0)\right]t^4 \\ +\left[\dfrac{84}{T^5}e_1(0) + \dfrac{-20}{T^4}\dot{e}_1(0) + \dfrac{10}{T^3}\ddot{e}_1(0) + \dfrac{1}{T^2}\dddot{e}_1(0)\right]t^5 + \left[\dfrac{-70}{T^6}e_1(0) + \dfrac{-20}{T^5}\dot{e}_1(0) + \dfrac{-7.5}{T^4}\ddot{e}_1(0) + \dfrac{-2}{T^3}\dddot{e}_1(0)\right]t^6 \\ +\left[\dfrac{20}{T^7}e_1(0) + \dfrac{-20}{T^6}\dot{e}_1(0) + \dfrac{2}{T^5}\ddot{e}_1(0) + \dfrac{1}{6T^4}\dddot{e}_1(0)\right]t^7, & 0 \le t \le T, \\ 0, & t \le T. \end{cases} \tag{30}$$

So, the forcing function can be calculated as

$$p_f(t) = c_1 p_1(t) + c_2 \dot{p}_1(t) + c_3 \ddot{p}_1(t). \tag{31}$$

The system described by equation (23) is reconstructed by the *U*-model method, which is influenced by the fluctuation of parameters and external disturbance. Considering the uncertainty of the model, equation (23) can be written as

$$\begin{cases} \dot{x}_1 = x_2, \\ \dot{x}_2 = x_3, \\ \dot{x}_3 = f'(\mathbf{x}) + d'(t) + g'(t)w(t), \end{cases} \tag{32}$$
$$y = x_1,$$

where $f'^{(\mathbf{x})} = -(\beta_2/\beta_3)x_3 - (\beta_1/\beta_3)x_2 - x_1$, $g'(t) = (1/\beta_3)[1 + \Delta(t)]$, $d'(t)$ represents the uncertainty caused by the perturbations of β_1, β_2, and β_3, and $\Delta(t)$ is the uncertainty of the input function, related to β_3. Assume these uncertainties bounded, i.e., $\|\Delta\| \le D_1$ and $\|d'(t)\| \le D_2$, where D_1 and D_2 are positive real numbers. Then, the controller can be designed as follows:

$$w(t) = -\beta_3\left[\frac{c_1}{c_3}(\dot{e}_1 - \dot{p}_1) + \frac{c_2}{c_3}(\ddot{e}_1 - \ddot{p}_1) + f'(\mathbf{x}) - \dddot{x}_{1d} - \dddot{p}_1 + \zeta \operatorname{sgn}(s)\right]. \tag{33}$$

Differentiating equation (27) and substituting equations (23) and (24) into it gives

$$\dot{s} = c_1(\dot{e}_1 - \dot{p}_1) + c_2(\ddot{e}_1 - \ddot{p}_1) + c_3 \cdot \left[f'(\mathbf{x}) + g'(t)w + \mathrm{d}'(t) - \dddot{x}_{1d} - \dddot{p}_1 \right]. \quad (34)$$

Then,

$$s\dot{s} = s\{c_1(\dot{e}_1 - \dot{p}_1) + c_2(\ddot{e}_1 - \ddot{p}_1) + c_3 \cdot \left[f'(\mathbf{x}) + g'(t)w + \mathrm{d}'(t) - \dddot{x}_{1d} - \dddot{p}_1 \right]\}. \quad (35)$$

Substituting $g\prime(t)$ and equation (33) into (35) yields

$$\begin{aligned} s\dot{s} &= s\left\{ c_3 \mathrm{d}'(t) + \Delta\left[c_3 \dddot{x}_{1d} + c_3 \dddot{p}_1 - c_1(\dot{e}_1 - \dot{p}_1) - c_2(\ddot{e}_1 - \ddot{p}_1) - c_3 f\prime(\mathbf{x}) \right] - (1+\Delta)c_3 \zeta \operatorname{sgn}(s) \right\} \\ &\le \|s\| \left[c_3 D_2 + D_1 \left\| c_3 \dddot{x}_{1d} + c_3 \dddot{p}_1 - c_1(\dot{e}_1 - \dot{p}_1) - c_2(\ddot{e}_1 - \ddot{p}_1) - c_3 f\prime(\mathbf{x}) \right\| - (1+\Delta)c_3\zeta \right] \\ &\le \|s\| \left[c_3 D_2 + D_1 \left\| c_3 \dddot{x}_{1d} + c_3 \dddot{p}_1 - c_1(\dot{e}_1 - \dot{p}_1) - c_2(\ddot{e}_1 - \ddot{p}_1) - c_3 f\prime(\mathbf{x}) \right\| - (1-D_1)c_3\zeta \right]. \end{aligned} \quad (36)$$

According to equation (36), when the switching control coefficient

$$\zeta \ge (1 - D_1)^{-1} \left[D_2 + D_1 \left\| \dddot{x}_{1d} + \dddot{p}_1 - \frac{c_1}{c_3}(\dot{e}_1 - \dot{p}_1) - \frac{c_2}{c_3}(\ddot{e}_1 - \ddot{p}_1) - f'(x) \right\| \right]. \quad (37)$$

the reaching condition $s\dot{s} \le 0$ can be satisfied, which means that the switching surface exists and the system will be stable. Therefore, utilizing equations (33) and (37), a global robust finite-time controller for the valve-controlled system can be determined.

In order to inhibit chattering, a boundary layer with thickness $\delta = 0.02$ for the quasi-sliding mode is specified, and a saturation function used for replacing the sign function is defined as

$$\operatorname{sat}(s) = \begin{cases} \operatorname{sgn}(s), & \|s\| > \delta, \\ \dfrac{s}{\delta}, & \|s\| < \delta. \end{cases} \quad (38)$$

Therefore, the nonlinear model controller from equation (33) can be rewritten as

$$w(t) = -\beta_3 \left[\frac{c_1}{c_3}(\dot{e}_1 - \dot{p}_1) + \frac{c_2}{c_3}(\ddot{e}_1 - \ddot{p}_1) + f'(\mathbf{x}) - \dddot{x}_{1d} - \dddot{p}_1 + \zeta \operatorname{sat}(s) \right]. \quad (39)$$

5. Simulation Studies

According to the above analyses, controller (39) can guarantee the reachability of the switching surface. If there is no disturbance and perturbation, the states of the system will follow (27) all the time, since the initial state is just on the switching surface. As the forcing function converges to zero in the time T, the valve-controlled system will become an error-free tracking system, which is a desirable result. However, for valve-controlled hydraulic systems, uncertainties always exist, such as fluctuation of external force, variation of elastic modulus with temperature, and inaccuracy of hydraulic oil density, which will firstly act on the solution of U-model and then affect the dynamic performance of the actual system. In addition, since digital controllers are widely applied now, the discretization of the control strategy will have an impact on the ultimate effect. In order to investigate these problems, the framework of the U-model-based finite-time control system and its simulation scheme are established, as shown in Figure 8.

Logically, the system includes an equivalent linear system and a global robust finite-time controller, and the connections between the two sections are a virtual control variable $w(k)$ and the state feedback $\mathbf{x}(k)$, while the actual physical controller should consist of the finite-time controller and the digital controller within the equivalent linear system. Therefore, this structure still embodies the U-model's thought of dealing with the nonlinear system in the controller.

In the simulation, assuming that the state vector $\mathbf{x}(k)$ is available in real time, the virtual control variable $w(k)$ can be calculated according to equation (39) and the digital controller in the equivalent linear system can be calculated according to equations (22) and (18). Exerting a standard sinusoidal signal $x_{1d} = \sin(t)$ as the command input on the system, the simulation is performed based on Simulink platform with the sampling period of 1 ms, as depicted in Figure 9. The parameters of the valve-controlled system are given by Table 1, and the simulation results are shown in Figure 10.

Simulation results show that the controller can track the position of the accurate nonlinear model of the valve-controlled cylinder hydraulic servosystem, and a U-model-based global robust finite-time controller described by Figure 8 is feasible. The valve-controlled system under the zero initial state can track the command signal within a specified time, and the transient process is quite smooth. Compared with the traditional PID controller, this method can eliminate the phase lag, as shown in Figure 11, which is

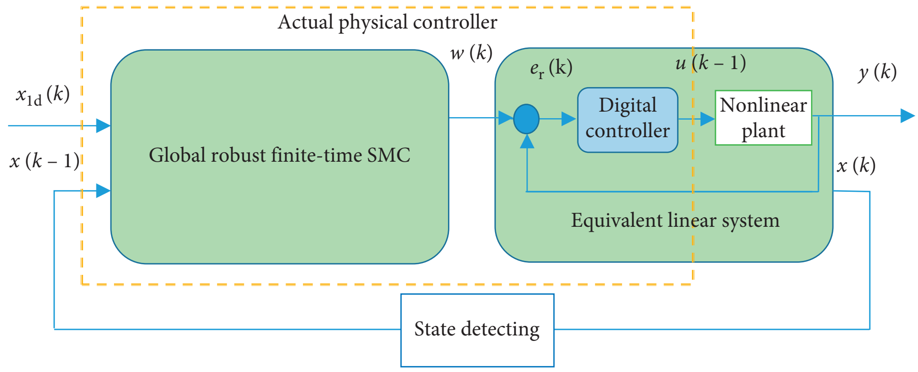

FIGURE 8: U-model-based global robust finite-time controller and simulation principle.

very important for some phase sensitive systems. In addition, this method effectively reduces the impact on the valve-controlled system at the beginning of the movement, as depicted in Figure 12.

On the basis of the U-model method and the proposed virtual nominal system, the nonlinear valve-controlled system has been redesigned as a linear system, so its controllability and performance are significantly improved. For example, the chattering of the switching function is greatly suppressed. Simulations show that if direct global robust finite-time control on this nonlinear valve-controlled system without U-model method is exerted, the chattering amplitude will be two orders of magnitude larger than that of the U-model-based control system, as shown in Figure 13. Moreover, when the U-model is adopted, the control error is greatly reduced after reaching the specified finite time, as shown in Figure 14.

Even so, the control error still exists in a small range and has the same periodicity as the command signal, indicating that the system is in a quasi-sliding mode state and the system itself is not strictly asymptotically stable. When the speed of the command signal increases, the phenomenon of the state, escaping from the sliding mode surface, is more obvious. In order to explore the essence of this issue, the simulation assumed that the valve-controlled system is ideal and there is no uncertainty. According to equation (34) and supposing that

$$\dot{s} = c_1(\dot{e}_1 - \dot{p}_1) + c_2(\ddot{e}_1 - \ddot{p}_1) + c_3 \cdot \left[f'(\mathbf{x}) + g'(t)w_{eq} + d'(t) - \dddot{x}_{1d} - \dddot{p}_1\right] = 0, \quad (40)$$

where w_{eq} is the equivalent control variable, then it gives

$$w_{eq} = -\beta_3\left[\frac{c_1}{c_3}(\dot{e}_1 - \dot{p}_1) + \frac{c_2}{c_3}(\ddot{e}_1 - \ddot{p}_1) + f'(\mathrm{x}) - \dddot{x}_{1d} - \dddot{p}_1\right]. \quad (41)$$

After replacing w with w_{eq} to drive the ideal system in Figure 8, run a simulation again, and the result, as shown in Figure 15(a), shows that although the system has fulfilled the tracking task, the value of the switching function still fluctuates with the command signal, which means that even if the system is under ideal conditions, its state cannot be always maintained on the switching surface. However, since w_{eq} is derived from equation (40), it should ensure that $\dot{s} \equiv 0$, but the actual $\dot{s}$ in the simulation is not constant, as depicted in Figure 15(b).

The analysis shows that the discretization of the controller brings the derivatives of x_{1d}, $\dot{x}_{1d}$, $\ddot{x}_{1d}$, p_1, $\dot{p}_1$, and $\ddot{p}_1$ different calculation errors, resulting in a minor mismatch with ideal equation (40). As w_{eq} is just calculated by (40), this mismatch can lead to the fluctuation of s and make the system unable to be asymptotically stable as expected. Therefore, this is an inherent error for the global robust sliding mode controller. However, for the specific application scenario of the valve-controlled hydraulic system, the maximum dynamic error has been restrained below 0.15% of the amplitude with the maximum speed of 1 m/s, which usually meets the requirements.

6. Conclusions

(1) Contrast to the traditional model of the valve-controlled hydraulic system, the new model structure has accommodated the nonlinear dynamics and the polarity effect of the control variable. Another insight on the nonlinear dynamic model is to use hyperbolic tangent function to approximate sign function for the relationship between pressure difference and spool displacement. Accordingly, these contributed make the theoretical model more consistent with the actual situation and provide a universal model structure for such system analysis and control design.

(2) By U-control design, the dynamic inversion of the controlled valve-controlled system can be achieved in real time, which makes the design of the control algorithm independent from the nonlinear characteristics of the system. On this basis, the proposed virtual nominal plant can not only eliminate the effect of the unfavorable high-frequency unmodeled dynamics and noise but also make it possible to adopt a ready-made control algorithm and obtain the same performance for different nonlinear plants.

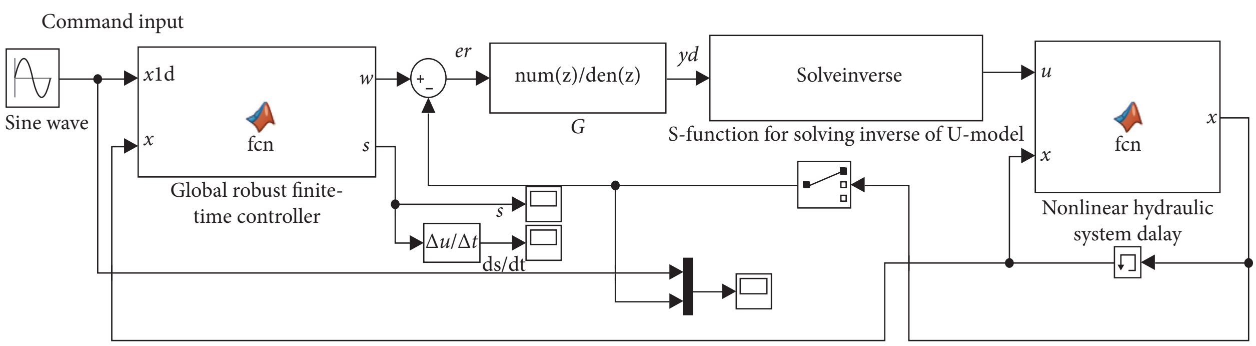

Figure 9: Simulation diagram by Simulink.

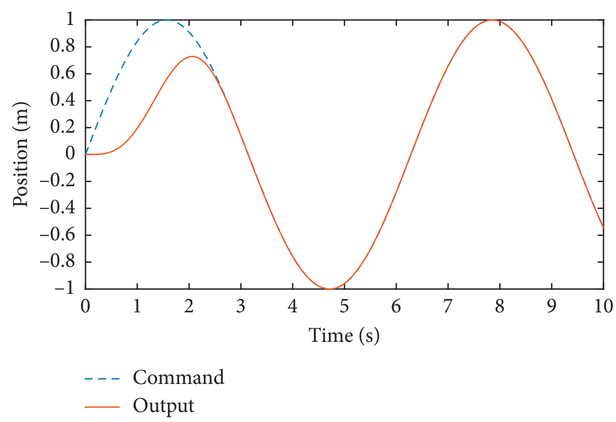

Figure 10: Simulation result of position tracking.

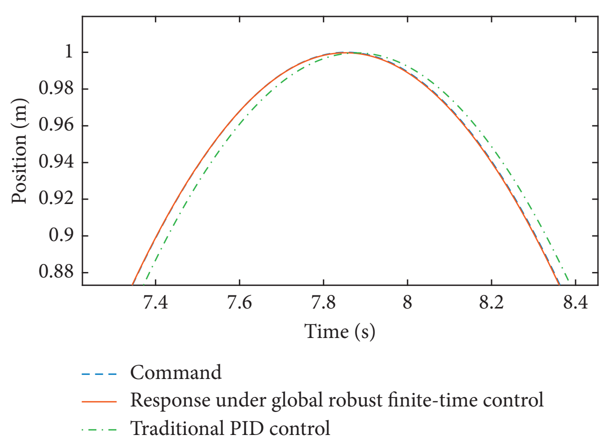

Figure 11: Comparison of different controllers.

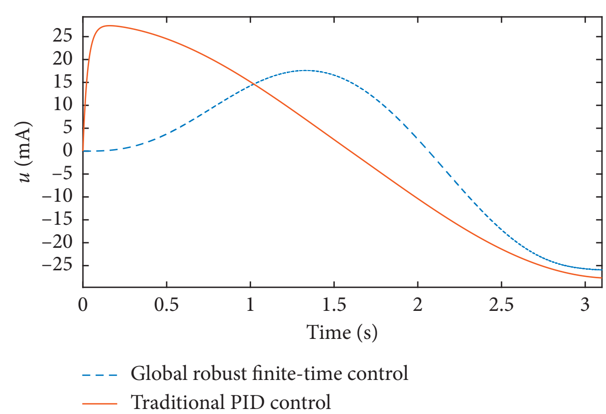

Figure 12: Impact of valve when motion starts.

Since the repeated design process can be omitted, the design efficiency is greatly enhanced.

(3) Meanwhile, the application of the virtual nominal plant changes the situation that the control variable cannot be expressed explicitly in the valve-controlled servosystem. Thus, the control variable is no longer considered as part of the uncertainty and the controlled plant is more regular; consequently, the control strategy can get better effect. With the U-model-based finite-time control method, the valve-controlled system can smoothly track the command signal within the specified time and the phase lag is eliminated, which is important for phase sensitive systems. Moreover, because of U-model's application, the chattering of the system effectively relieved and the control error greatly reduced.

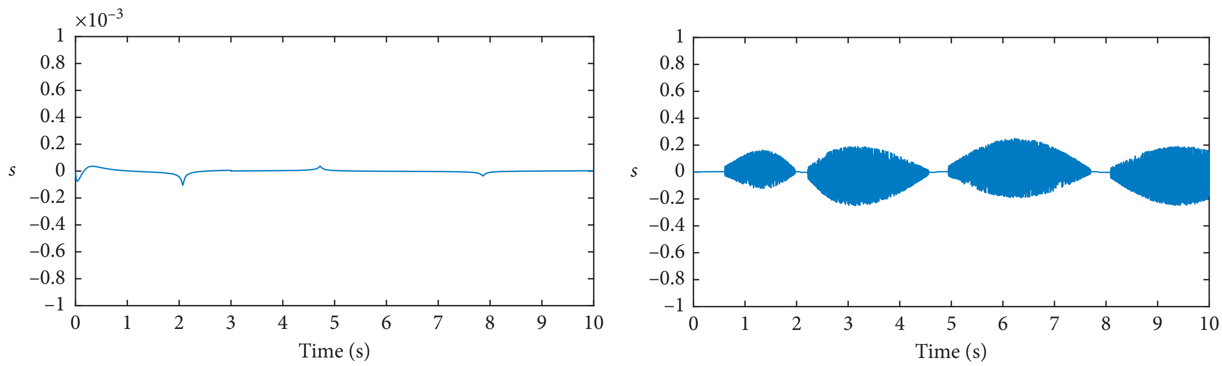

(a) (b)

Figure 13: Smoothness of the switching function for global robust finite-time control: (a) U-model-based control and (b) direct control without U-model.

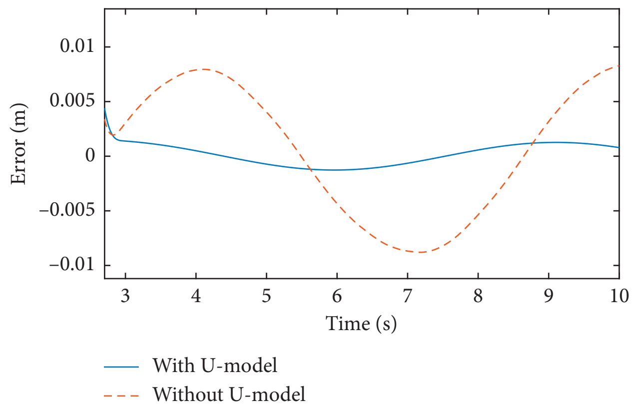

Figure 14: Dynamic control error.

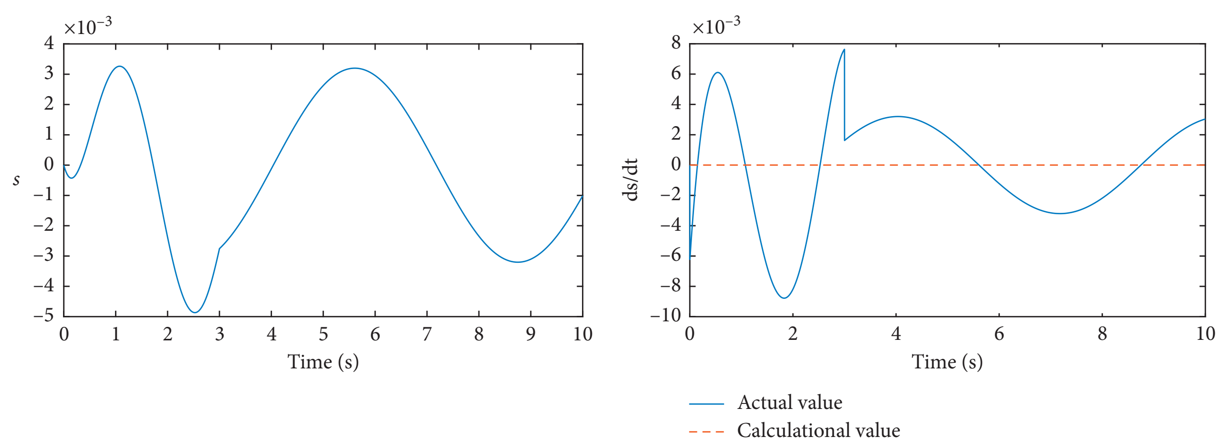

(a) (b)

Figure 15: Simulated switching function value for ideal valve-controlled system under equivalent control. (a) Value of s. (b) Value of $\dot{s}$.

(4) The discretization will cause the system state to fluctuate near the switching surface with the speed's variation, resulting in a certain dynamic error. However, for the specific application scenario of the valve-controlled system, the dynamic error can be maintained below 0.15% of the amplitude with the maximum speed of 1 m/s, which usually can meet the requirements.

Data Availability

The data used to support the findings of this study are available from the corresponding author upon request.

Disclosure

This work was completed when the first author was an academic visitor at the University of the West of England.

Conflicts of Interest

The authors declare that they have no conflicts of interest.

Acknowledgments

This work was funded by the National Natural Science Foundation of China (Grant no. 51775032), Foundation of Key Laboratory of Vehicle Advanced Manufacturing, Measuring and Control Technology, Beijing Jiaotong University, Ministry of Education, China, and China Scholarship Council.

References

[1] H. E. Merritt, *Hydraulic Control Systems*, Wiley, New York, NY, USA, 1991.

[2] H. R. Li, *Hydraulic Control System*, National Defense Industry Press, Beijing, China, 1991.

[3] C. X. Wang, *Hydraulic Control System*, China Machine Press, Beijing, China, 2011.

[4] M. Galicki, "Finite-time control of robotic manipulators," *Automatica*, vol. 51, pp. 49–54, 2015.

[5] M. Galicki, "Constraint finite-time control of redundant manipulators," *International Journal of Robust and Nonlinear Control*, vol. 27, no. 4, pp. 639–660, 2016.

[6] J. Zhang, Q. Hu, and D. Wang, "Bounded finite-time attitude tracking control for rigid spacecraft via output feedback," *Aerospace Science and Technology*, vol. 64, pp. 75–84, 2017.

[7] J.-G. Sun, S.-L. Xu, S.-M. Song, and X.-J. Dong, "Finite-time tracking control of hypersonic vehicle with input saturation," *Aerospace Science and Technology*, vol. 71, pp. 272–284, 2017.

[8] H. Pan, X. Jing, and W. Sun, "Robust finite-time tracking control for nonlinear suspension systems via disturbance compensation," *Mechanical Systems and Signal Processing*, vol. 88, pp. 49–61, 2017.

[9] X. H. Ye, *Research on Modelling and Control Method of Valve-Controlled Asymmetrical Cylinder System*, Hefei University of Technology, Hefei, China, 2015.

[10] L. Li, F. Li, Y. B. Feng et al., "Research on control strategy of large hydraulic erecting system based on adaptive fuzzy sliding mode," *Acta Armamentarii*, vol. 37, no. 1, pp. 71–76, 2016.

[11] Y. Li, L. M. Yang, and Z. H. Zhang, "Study on sencond-order sliding mode control law for electro-hydraulic servo system," *Chinese Journal of Mechanical Engineering*, vol. 41, no. 3, pp. 72–75, 2005.

[12] L. Schmidt, T. O. Andersen, and H. C. Pedersen, "An approach for second order control with finite time convergence for electro-hydraulic drives," in *Proceedings of the ASME/BATH 2013 Symposium on Fluid Power & Motion Control*, American Society of Mechanical Engineers (ASME), Sarasota, FL, USA, October 2013.

[13] J. Y. Yao, L. Liu, H. Jian et al., "Finite time continuous sliding mode control method for electro-hydraulic position servo system," Chinese Patent CN105093936A, 2015.

[14] Q. M. Zhu and L. Z. Guo, "A pole placement controller for non-linear dynamic plants," *Proceedings of the Institution of Mechanical Engineers, Part I: Journal of Systems and Control Engineering*, vol. 216, no. 6, pp. 467–476, 2002.

[15] Q. M. Zhu, D. Y. Zhao, and J. Zhang, "A general U-block model-based design procedure for nonlinear polynomial control systems," *International Journal of Systems Science*, vol. 47, no. 14, pp. 3465–3475, 2016.

[16] F. X. Xu, Q. M. Zhu, D. Y. Zhao et al., "*U*-model based design methods for nonlinear control systems: a survey of the development in the 1st decade," *Control and Decision*, vol. 28, no. 7, pp. 961–971, 2013.

[17] S. A. Billings, *Nonlinear System Identification: NARMAX Methods in the Time, Frequency, and Spatio-Temporal Domains*, Wiley, New York, NY, USA, 2013.

[18] Y.-S. Lu and J.-S. Chen, "Design of a global sliding-mode controller for a motor drive with bounded control," *International Journal of Control*, vol. 62, no. 5, pp. 1001–1019, 1995.